

C_{60} cation as the carrier of the $\lambda 9577$ Å and $\lambda 9632$ Å diffuse interstellar bands: Further support from the VLT/X-Shooter spectra

T.P. Nie^{1,2}, F.Y. Xiang^{1,2*}, and Aigen Li^{2†}

¹Hunan Key Laboratory for Stellar and Interstellar Physics and School of Physics and Optoelectronics, Xiangtan University, Hunan 411105, China

²Department of Physics and Astronomy, University of Missouri, Columbia, MO 65211, USA

ABSTRACT

Ever since their first detection over 100 years ago, the mysterious diffuse interstellar bands (DIBs), a set of several hundred broad absorption features seen against distant stars in the optical and near infrared wavelength range, largely remain unidentified. The close match both in wavelengths and in relative strengths recently found between the experimental absorption spectra of gas-phase buckminsterfullerene ions (C_{60}^+) and four DIBs at $\lambda 9632$ Å, $\lambda 9577$ Å, $\lambda 9428$ Å and $\lambda 9365$ Å (and, to a lesser degree, a weaker DIB at $\lambda 9348$ Å) suggests C_{60}^+ as a promising carrier for these DIBs. However, arguments against the C_{60}^+ identification remain and are mostly concerned with the large variation in the intensity ratios of the $\lambda 9632$ Å and $\lambda 9577$ Å DIBs. In this work we search for these DIBs in the ESO VLT/X-shooter archival data and identify the $\lambda 9632$ Å, $\lambda 9577$ Å, $\lambda 9428$ Å, and $\lambda 9365$ Å DIBs in a sample of 25 stars. While the $\lambda 9428$ Å and $\lambda 9365$ Å DIBs are too noisy to allow any reliable analysis, the $\lambda 9632$ Å and $\lambda 9577$ Å DIBs are unambiguously detected and, after correcting for telluric water vapor absorption, their correlation can be used to probe their origin. To this end, we select a subsample of nine hot, O- or B0-type stars of which the stellar MgII contamination to the $\lambda 9632$ Å DIB is negligibly small. We find that their equivalent widths, after normalized by reddening to eliminate their common correlation with the density of interstellar clouds, exhibit a tight, positive correlation, supporting C_{60}^+ as the carrier of the $\lambda 9632$ Å and $\lambda 9577$ Å DIBs.

Key words: ISM: dust, extinction — ISM: lines and bands — ISM: molecules

1 INTRODUCTION

The diffuse interstellar bands (DIBs) are a series of over 600 broad absorption bands seen in the optical and near infrared (IR) spectra of stars as the starlight passes through the diffuse interstellar clouds (Sarre 2006, Fan et al. 2019, McCabe 2019, Linnartz et al. 2020). They were first observed in 1919 at 5780 Å and 5797 Å in the spectrum of the distant supergiant ζ Persei by Mary Lea Heger (1922), a then graduate student at Lick Observatory, and nearly two decades later, the interstellar origin of these bands was established by Merrill & Wilson (1938), based on the strong correlation between the band strength and the interstellar reddening.

Almost every article on DIBs started by stating that, “... since the discovery that DIBs are interstellar”, as Désert

et al. (1995) put it, “the nature of their carriers is still unknown”. This remained true until Campbell et al. (2015, 2016a,b), Walker et al. (2015, 2017) and Campbell & Maier (2018) for the first time measured the gas-phase spectrum of buckminsterfullerene cation (C_{60}^+) and found that the spectral characteristics (i.e., wavelengths and relative strengths) of gas-phase C_{60}^+ are in agreement with four DIBs at $\lambda 9365.2$ Å, $\lambda 9427.8$ Å, $\lambda 9577.0$ Å, and $\lambda 9632.1$ Å, arguably as well as a weaker DIB at $\lambda 9348.4$ Å. Further support for this identification was provided by space observations obtained with the *Hubble Space Telescope* (HST) which were free of telluric absorption contamination (Cordiner et al. 2019).

The original idea of C_{60}^+ being a possible DIB carrier dates back to the pioneering work by Foing & Ehrenfreund (1994), who linked the neon/argon matrix spectra of C_{60}^+ recorded by Fulara et al. (1993) to two strong DIBs at $\lambda 9577$ Å and $\lambda 9632$ Å. A direct comparison was not possi-

* fyxiang@xtu.edu.cn

† lia@missouri.edu

ble, though, because the inert gas matrix environment would broaden the band widths and shift the wavelengths. More recently, the presence of C_{60}^+ in the interstellar medium (ISM) has been revealed through the detections of the 6.4, 7.1, 8.2 and 10.5 μm emission features of C_{60}^+ in reflection nebulae, planetary nebulae and the Large and Small Magellanic Clouds (Berné et al. 2013, Strel'nikov et al. 2015). These detections may not be too surprising, as its parent molecule C_{60} , first experimentally synthesized by Kroto et al. (1985), has also been detected in various astrophysical environments through its characteristic IR emission features at 7.0, 8.45, 17.3 and 18.9 μm (Cami et al. 2010; Sellgren et al. 2010; García-Hernández et al. 2010, 2011; Zhang & Kwok 2011).

If the $\lambda 9348 \text{ \AA}$, $\lambda 9365 \text{ \AA}$, $\lambda 9428 \text{ \AA}$, $\lambda 9577 \text{ \AA}$, and $\lambda 9632 \text{ \AA}$ DIBs indeed share the same carrier and arise from C_{60}^+ , their strengths should correlate. Although the assignment of these five DIBs to C_{60}^+ has gained wide acceptance, challenge has been continuously posed. Particularly, the intensity ratio of the two strongest bands of C_{60}^+ at 9577 and 9632 \AA has become a topic of discussion. While the laboratory spectrum of gas-phase C_{60}^+ indicates an intensity ratio of ~ 0.84 for the 9632 \AA band to the 9577 \AA band (Campbell & Maier 2018), Galazutdinov et al. (2017) found that, after correcting for the MgII stellar contamination through model atmosphere calculations, the ratio of the equivalent width of the $\lambda 9632 \text{ \AA}$ DIB to that of $\lambda 9577 \text{ \AA}$ DIB is variable within a broad range. Given that both the 9632 \AA band and the 9577 \AA band of C_{60}^+ originate from electronic transitions starting from the same level in the ^2Au ground state (but also see Lykhin et al. 2019, Hrodmarsson et al. 2020), such a varying value is not a priori expected. As a result, Galazutdinov et al. (2017) argued against the assignment of the $\lambda 9577 \text{ \AA}$ and $\lambda 9632 \text{ \AA}$ DIBs to C_{60}^+ since their relative strengths are too poorly correlated to be caused by a single source. Using close spectral standards to correct for the MgII stellar contamination, Walker et al. (2017) examined some of the same spectra of Galazutdinov et al. (2017) and found that, within the uncertainties, the $\lambda 9577 \text{ \AA}$ and $\lambda 9632 \text{ \AA}$ DIBs are somewhat correlated. They further argued that the use of close spectral standards is superior to model atmosphere calculations in correcting for contamination by the MgII stellar lines. More recently, Galazutdinov et al. (2021) again reported a lack of correlation between the equivalent widths of the $\lambda 9577 \text{ \AA}$ and $\lambda 9632 \text{ \AA}$ DIB for a sample of 43 stars.

To test the C_{60}^+ assignment of DIBs, we search for these DIBs in the ESO VLT/X-shooter archival spectra and examine their interrelations. We base on the ESO VLT/X-shooter archival data and identify the $\lambda 9577 \text{ \AA}$ and $\lambda 9632 \text{ \AA}$ DIBs superimposed on the stellar spectra of a number of stars. We find that their strengths are well correlated and therefore provide further support for the C_{60}^+ assignment of DIBs. This paper is organized as follows. We first briefly describe in §2 the ESO VLT/X-shooter data set. In §3 we report and discuss the results on the DIB search and measure the DIB strengths, and also explore their correlations. The major conclusions are summarized in §4.

2 ESO VLT/X-SHOOTER SPECTRAL DATA PRODUCTS

The X-shooter is the first of the 2nd generation instruments installed on the *European Southern Observatory* (ESO) *Very Large Telescope* (VLT). It is a very efficient single-target, medium-resolution spectrometer ($R \sim 4,000\text{--}17,000$), covering the spectral range from 300 to 2,500 nm in a single exposure (Vernet et al. 2011). We searched for the $\lambda 9348 \text{ \AA}$, $\lambda 9365 \text{ \AA}$, $\lambda 9428 \text{ \AA}$, $\lambda 9577 \text{ \AA}$, and $\lambda 9632 \text{ \AA}$ DIBs from the X-shooter archival spectra in the ESO Spectral Data Products.¹ We found 25 stars which simultaneously exhibit the $\lambda 9365 \text{ \AA}$, $\lambda 9428 \text{ \AA}$, $\lambda 9577 \text{ \AA}$ and $\lambda 9632 \text{ \AA}$ DIBs. The $\lambda 9348 \text{ \AA}$ DIB, the weakest band in the experimental absorption spectrum of gas-phase C_{60}^+ (Campbell et al. 2015, Walker et al. 2017, Campbell & Maier 2018), is not seen in the X-shooter spectra. This does not necessarily mean that the $\lambda 9348 \text{ \AA}$ DIB is absent; instead, it may merely be weak enough to have escaped detection.

It is interesting to note that Galazutdinov et al. (2017) reported the nondetection of the three weak absorption bands of C_{60}^+ at 9348, 9365 and 9428 \AA in a sample of 19 heavily reddened interstellar sight lines observed from the ground at high signal-to-noise (S/N). The apparent absence of these weak bands in sight lines where the $\lambda 9577 \text{ \AA}$ and $\lambda 9632 \text{ \AA}$ bands are strong casts strong doubt on the C_{60}^+ assignment.² However, the wavelength region where the weak absorption bands of C_{60}^+ occur is heavily contaminated in ground-based studies due to strong telluric absorption. To circumvent the telluric contamination issues, Cordiner et al. (2019) obtained high S/N, telluric free HST spectra of seven heavily reddened stars and reported unambiguous detections of two weak bands at 9365 and 9428 \AA . and one strong band at 9577 \AA . The intensity ratios of the $\lambda 9577 \text{ \AA}$, $\lambda 9428 \text{ \AA}$, and $\lambda 9365 \text{ \AA}$ DIBs measured for early B stars were about 1.0:0.08:0.23, comparable to the experimental ratios of 1.0:0.15:0.25 derived from the laboratory spectrum of C_{60}^+ (see Cordiner et al. 2019). Unfortunately, the HST *Space Telescope Imaging Spectrograph* (STIS) grating setting adopted by Cordiner et al. (2019) did not allow them to survey the $\lambda 9632 \text{ \AA}$ DIB. Therefore, it is not possible to analyze the relation between the $\lambda 9577 \text{ \AA}$ and $\lambda 9632 \text{ \AA}$ DIBs based on the telluric free HST/STIS spectra.

As mentioned earlier, there are large numbers of telluric water vapor absorption lines in the wavelength range of C_{60}^+ bands. We employ Molecfit to correct X-shooter archive data products for telluric absorption. Molecfit is a tool to correct

¹ We note that in the literature these DIBs have been detected and their strengths have been reported for a number of sources. We prefer to search for these DIBs in archival data and derive their strengths by ourselves. This is because in the literature there is a certain arbitrariness in defining the continuum against the DIB absorption and the DIB strengths were often measured in different ways. When taking data from different sources, these differences actually play a role.

² As noted by Linnartz et al. (2020), while Walker et al. (2015, 2016) reported the detection of three weak DIBs at 9348, 9365 and 9428 \AA which coincide with the weak absorption features seen in the gas-phase spectrum of C_{60}^+ , these DIBs were not observed *simultaneously* along one line of sight, but merely complementary towards different targets. See Lallement et al. (2018) for an overview of the detectability of the DIBs attributed to C_{60}^+ .

Table 1. Stellar Parameters and the Equivalent Widths of the $\lambda 9577 \text{ \AA}$ DIB (W_{9577}) and $\lambda 9632 \text{ \AA}$ DIB (W_{9632}) for Our Sample of Nine Stars in the VLT/X-Shooter Archive

Target Star	Spectral Type	T_{eff} (K)	B^a (mag)	V^a (mag)	$(B - V)_0^b$ (mag)	$E(B - V)$ (mag)	W_{9577} (mÅ)	W_{9632} (mÅ)
2MASS J17253421-3423116	O5.5IV ^c	40,000	13.53	11.82	-0.29	2.00 ^d	385.8±46.5	379.2±32.3
4U1907+09	O8.5Iab ^c	33,000	19.41	16.35	-0.27	3.33 ^d	349.2±36.4	278.8±7.4
Cl Pismis 24 17	O3.5III ^c	44,000	13.33	11.84	-0.26	1.75 ^d	314.1±8.6	384.7±13.8
B111	O4.5V ^e	42,850 ^e	—	—	—	1.35 ^e	384.1±52.8	392.0±18.7
B150	B0V ^f	30,000	—	—	—	1.32 ^f	497.8±41.6	492.6±29.0
B164	O6Vz ^e	39,100 ^e	—	—	—	1.76 ^e	557.5±7.3	544.1±24.0
B215	B0-B1V ^e	28,000 ^e	—	—	—	1.85 ^e	466.1±77.8	423.1±10.7
B289	O9.7V ^e	33,800 ^e	—	—	—	1.73 ^e	570.9±57.5	436.7±21.3
B311	O8.5Vz ^e	35,950 ^e	—	—	—	1.62 ^e	699.7±55.0	645.7±24.6

^a B and V photometric magnitudes taken from <http://cdsportal.u-strasbg.fr/>.

^b Intrinsic colors $(B - V)_0$ taken from Wegner (2014).

^c Stellar spectral types adapted from <http://cdsportal.u-strasbg.fr/>.

^d Color excesses $E(B - V) \equiv (B - V) - (B - V)_0$.

^e Ramírez-Tannus et al. (2018).

^f Nielbock et al. (2001).

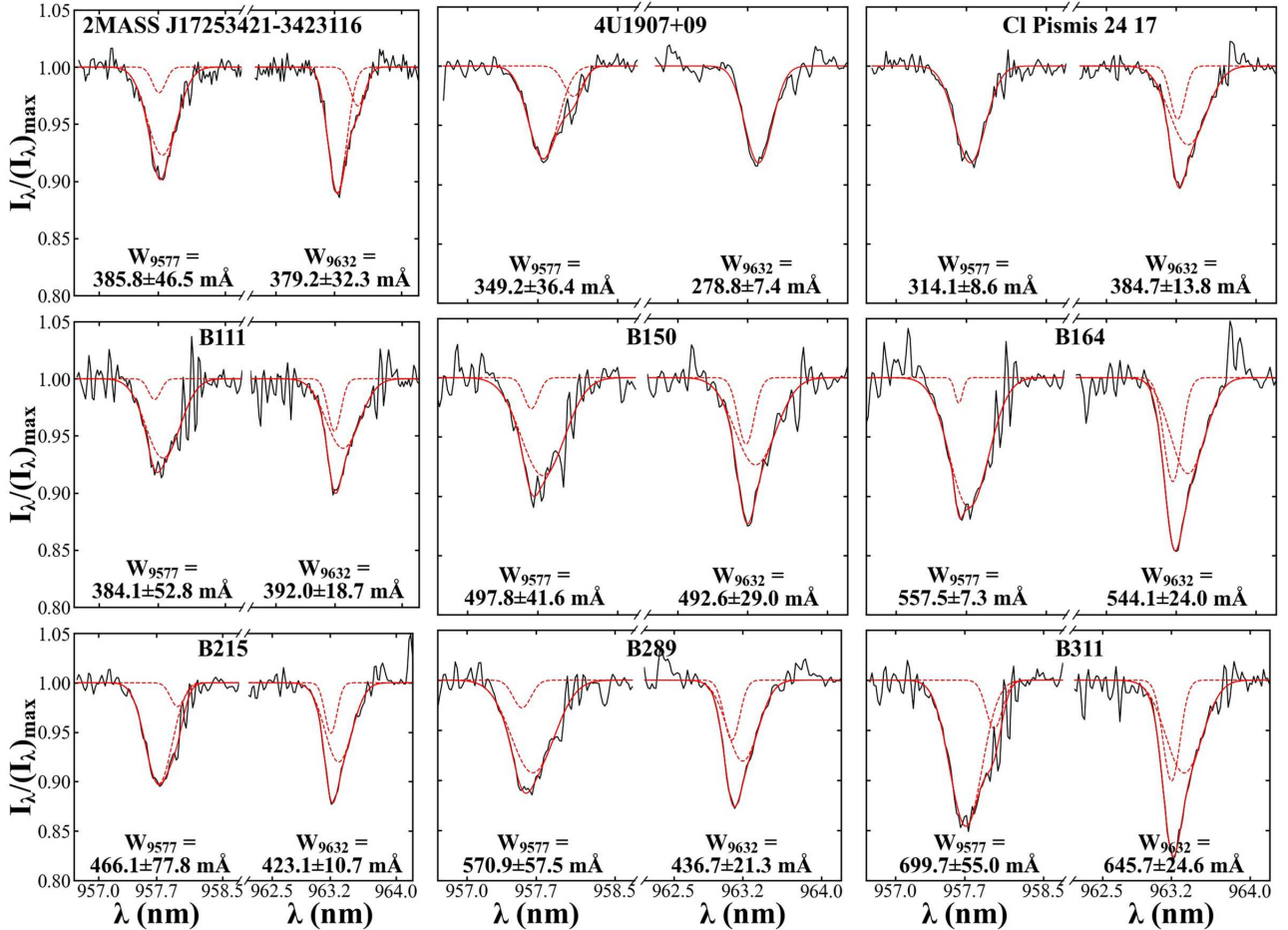


Figure 1. The $\lambda 9577 \text{ \AA}$ and $\lambda 9632 \text{ \AA}$ DIBs (solid black lines) seen in the VLT/X-shooter spectra of nine target stars. Each DIB is fitted either by a single Gaussian profile or by a combination of two Gaussian profiles. The solid red lines show the fitted profiles, while the dotted red lines show the Gaussian fitting components. Labeled in each panel are the DIB equivalent widths.

for telluric absorption lines based on synthetic modeling of the atmospheric transmission which can be used with data obtained with various ground-based telescopes and instruments (Smette et al. 2015, Kausch et al. 2015). Also, the $\lambda 9632$ Å DIB coincides and therefore often blends with the stellar MgII absorption lines at 9631.9 and 9632.4 Å. However, it is far from trivial to correct for contamination by the stellar MgII lines. Nevertheless, it is well recognized that while the stellar MgII lines are strong in late B stars, they are negligibly weak in hot, O- and early B-type stars of effective temperatures $T_{\text{eff}} \gtrsim 20,000$ K (e.g., see Figure 2 of Galazutdinov et al. 2017). Therefore, we focus on a subsample of nine stars which consists of seven O stars and two B0 stars (see Table 1). In Figure 1 we show the X-shooter spectra of the $\lambda 9577$ Å and $\lambda 9632$ Å DIBs of these stars. To verify that these stars are indeed weak in MgII absorption, we show in Figure 2 their MgII stellar absorption line at 4481 Å. Except for 2MASS J17253421-3423116 for which there is no X-shooter data around 4481 Å, the 4481 Å MgII stellar line is indeed either absent or very weak in all the other eight stars. Therefore, the correction for stellar contamination by MgII to the $\lambda 9632$ Å DIB is unnecessary for our stars of which the effective temperatures all exceed 28,000 K.

3 THE $\lambda 9577$ Å AND $\lambda 9632$ Å DIBS AND THEIR CORRELATIONS

As described in §2, although the X-shooter spectra of our target stars show evidence for the presence of all four DIBs at $\lambda 9365$ Å, $\lambda 9428$ Å, $\lambda 9577$ Å and $\lambda 9632$ Å DIBs, the spectral profiles of the $\lambda 9365$ Å and $\lambda 9428$ Å DIBs are too noisy to allow for any reliable quantitative analysis. In contrast, as shown in Figure 1, the $\lambda 9577$ Å and $\lambda 9632$ Å DIBs, the strongest absorption features in the experimental spectrum of gas-phase C_{60}^+ (Campbell et al. 2015, Walker et al. 2017, Campbell & Maier 2018), are unambiguously detected in the X-shooter spectra. As mentioned earlier, the stellar MgII absorption lines which would pollute the $\lambda 9632$ Å DIBs are absent or very weak in hot O- and early B-type stars. We therefore confine ourselves to nine O and B0 stars along the lines of sight to which the stellar MgII contamination is negligible. After correcting for the telluric contamination with the Molecfit tool, we fit the absorption profiles of the $\lambda 9577$ Å and $\lambda 9632$ Å DIBs by a single Gaussian profile or a combination of two Gaussian profiles.³ The $\lambda 9577$ Å and $\lambda 9632$ Å DIB profiles are often asymmetrical, therefore a single Gaussian profile is often not sufficient and two or more Gaussian profiles are required to closely reproduce the observed DIB profiles (e.g., see Rawlings et al. 2014). Indeed, as shown in Figure 1, a combination of two Gaussian profiles are needed for the majorities of the target stars (8/9 for both DIBs). In principle, we could also fit the DIB profiles in terms of

³ We are only interested in the DIB band strength (i.e., the area obtained by integrating the absorption band over wavelength) and thus the exact functional profile adopted to fit the band is not critical. We have actually also tried to fit the DIB absorption bands in terms of Lorentzian or Drude profiles which are expected for damped harmonic oscillators (see Li 2009). However, both Lorentzian and Drude profiles are too broad in the blue and red wings to reproduce the DIB absorption bands.

one or two Lorentzian functions. This really does not matter since we are only interested in the area integrated over the DIB absorption profile.

We determine the absorption strengths of the $\lambda 9577$ Å and $\lambda 9632$ Å DIBs from the fitted Gaussian profile(s) in terms of their equivalent widths, W_{9577} and W_{9632} . The equivalent width of a DIB is a measure of the DIB absorption strength which characterizes the “width” of a “virtual” rectangle whose area is equal to the area in the DIB profile and whose height is equal to the continuum level of the DIB profile. We tabulate in Table 1 the measured equivalent widths (W_{9577} , W_{9632}) and their associated uncertainties of the $\lambda 9577$ Å and $\lambda 9632$ Å DIBs for the nine target stars.

If C_{60}^+ indeed causes both the $\lambda 9577$ Å and $\lambda 9632$ Å DIBs, their equivalent widths should correlate. While a good correlation between two DIBs does not necessarily mean that they must share a common carrier, a non-correlation implies that different carriers are involved (e.g., see Moutou et al. 1999). We conduct a correlation analysis on W_{9577} and W_{9632} to investigate whether the $\lambda 9577$ Å and $\lambda 9632$ Å DIBs are related, so as to determine whether they are from the same carrier (e.g., C_{60}^+). As illustrated in Figure 3a, with a Pearson correlation coefficient of $r \approx 0.89$ and a Kendall correlation coefficient of $\tau \approx 0.72$ at a significance level of $p \approx 1.32 \times 10^{-3}$, it is apparent that W_{9577} and W_{9632} are well correlated. The correlation coefficient becomes $r \approx 0.96$ when the measurement uncertainties are taken into account.

On average, the strength ratio of the $\lambda 9632$ Å DIB to the $\lambda 9577$ Å DIB is ~ 0.94 , which agrees reasonably well with that of the experimental spectrum of gas-phase C_{60}^+ (~ 0.84 , Campbell & Maier 2018). The discrepancy of $\sim 12\%$ between the observed ratio of $W_{9632}/W_{9577} \approx 0.94$ and the experimental ratio of $W_{9632}/W_{9577} \approx 0.84$ is acceptable. We note that the reported experimental intensity ratio was not for pure C_{60}^+ , but actually for small He-tagged $\text{C}_{60}^+-\text{He}_n$ ($n = 1-3$) ion complexes in an ion trap (Campbell & Maier 2018). Upon tagged by He atoms, the laboratory rest wavelengths of C_{60}^+ are slightly redshifted. As the redshift is linearly dependent on the number of He atoms (see Gatchell et al. 2019), the absorption wavelengths of bare C_{60}^+ can be extrapolated from that of $\text{C}_{60}^+-\text{He}_n$ complexes (e.g., see Campbell et al. 2016b, Spieler et al. 2017).⁴ The absence of actual data for bare C_{60}^+ still leaves a concern about the exact W_{9632}/W_{9577} intensity ratio. Moreover, even the nature of the electronic transitions responsible for the 9632 and 9577 Å absorption bands seen in C_{60}^+ remains unknown (e.g., see Lykhin et al. 2019, Hrodmarsson et al. 2020).

Nevertheless, as mentioned earlier, such a correlation between W_{9577} and W_{9632} does not necessarily mean that the $\lambda 9577$ Å and $\lambda 9632$ Å DIBs must arise from the same carrier. The equivalent widths of two DIBs resulting from different carriers for a random sample of lines of sight may somewhat correlate *if* their carriers are present in the interstellar medium (ISM) of different lines of sight in proportional abundances. In general, most interstellar quantities show a linear increase with the densities of the in-

⁴ The linear dependence of the wavelength redshift on the number of tagged He atoms remains valid up to 32 He atoms. From 33 He atoms onwards the redshift is not linear anymore (see Gatchell et al. 2019).

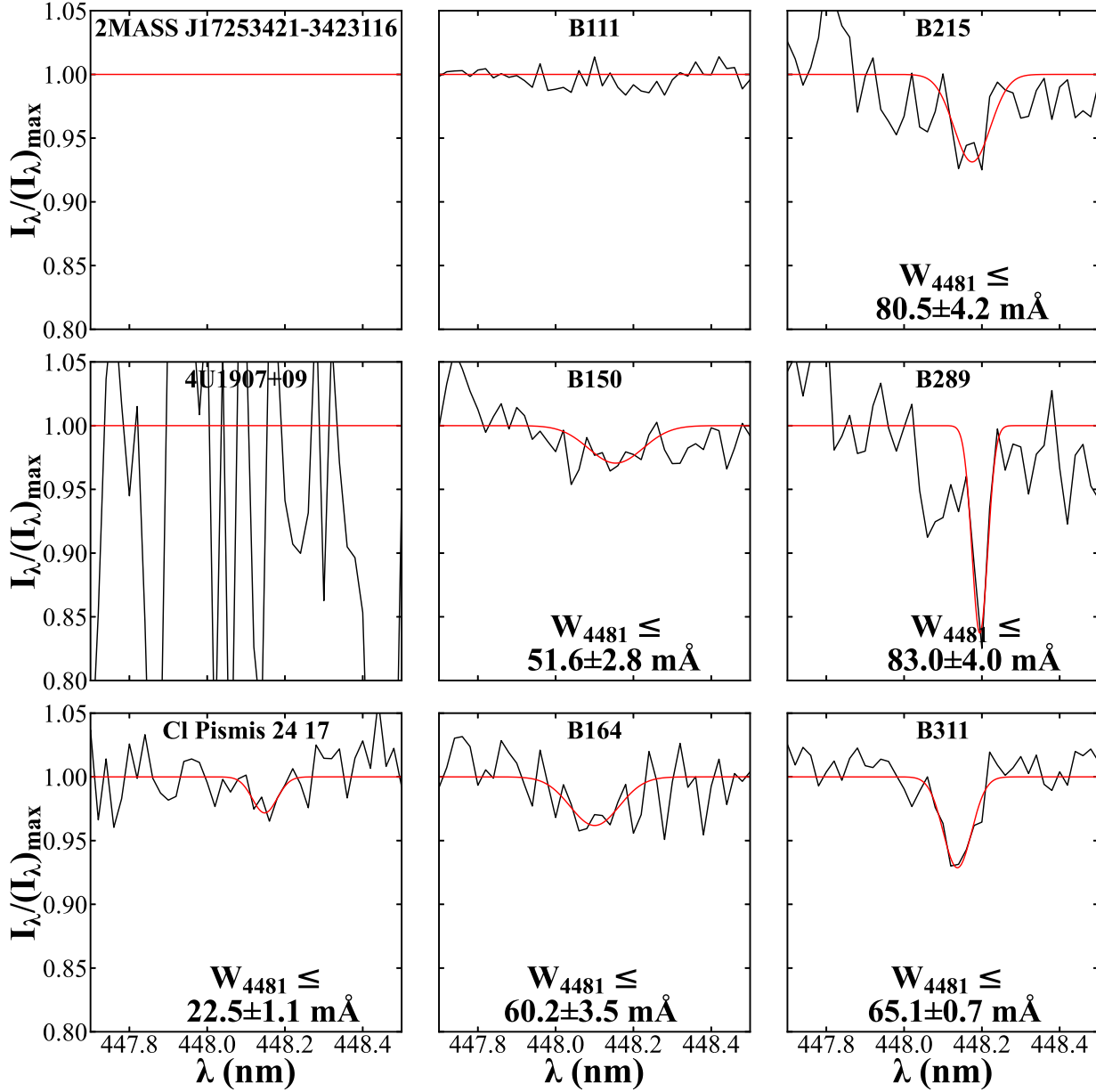


Figure 2. The stellar MgII line at 4481 \AA is absent or very weak in the X-shooter spectra (solid black line) of our target stars. For 2MASS J17253421-3423116, there is no X-shooter data. For 4U1907+09, the X-shooter spectrum is too noisy. Labeled in each panel is the equivalent width of the 4481 \AA stellar MgII line.

terstellar clouds measured by gas, e.g., the hydrogen column density N_{H} , or by dust, e.g., the interstellar reddening $E(B - V)$ or extinction A_V (e.g., see Witt et al. 1983; Seab & Snow 1984; Fitzpatrick & Massa 1988; Moutou et al. 1999; Xiang et al. 2011, 2017; Li et al. 2019). The correlation between two DIBs may only indicate the coexistence of two separate agents in the ISM, of which the abundances both are correlated with N_{H} or $E(B - V)$. Indeed, it is long recognized that the DIB strengths are correlated with the interstellar reddening $E(B - V)$. To eliminate the common correlation with $E(B - V)$, we therefore normalize the DIB equivalent widths by $E(B - V)$ and examine the correlation between $W_{9577}/E(B - V)$ and $W_{9632}/E(B - V)$. As shown in Figure 3b, with a Pearson correlation coef-

ficient of $r \approx 0.95^5$ and a Kendall correlation coefficient of $\tau \approx 0.83$ at a significance level of $p \approx 8.08 \times 10^{-5}$, $W_{9577}/E(B - V)$ and $W_{9632}/E(B - V)$ are clearly well correlated. This supports that a common carrier is at the origin of the $\lambda 9577 \text{ \AA}$ and $\lambda 9632 \text{ \AA}$ DIBs. We derive a mean ratio of $W_{9632}/E(B - V) : W_{9577}/E(B - V) \approx 0.95$, which also agrees reasonably well with the experimental band ratio of gas-phase C_{60}^+ (~ 0.84 , Campbell & Maier 2018).

Finally, we note that Galazutdinov et al. (2021) compiled the spectral data of 43 lines of sight for the $\lambda 9577 \text{ \AA}$ and $\lambda 9632 \text{ \AA}$ DIBs obtained with different instruments on

⁵ The correlation coefficient essentially remains unchanged when the measurement uncertainties are taken into account.

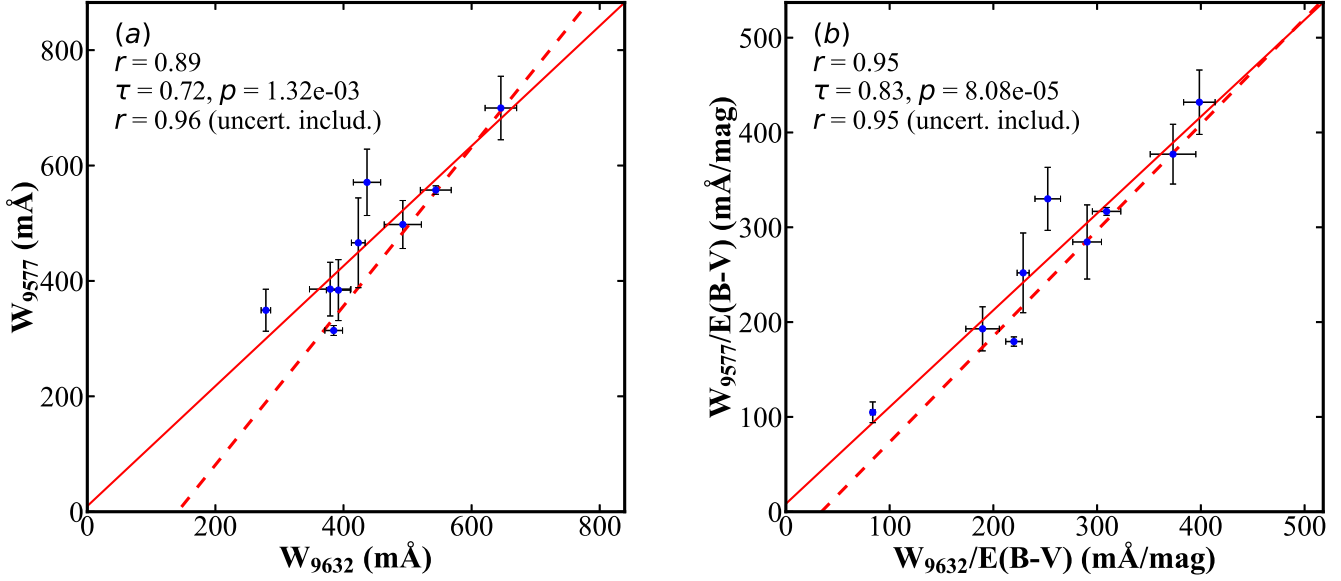


Figure 3. Left panel (a): Correlation diagram of the equivalent widths of the $\lambda 9577$ Å DIB with that of the $\lambda 9632$ Å DIB seen in our sample of nine target stars. Right panel (b): Correlation diagram of the *reddening-normalized* equivalent widths of the $\lambda 9577$ Å DIB with that of the $\lambda 9632$ Å DIB for our sample of nine stars. Labeled in both panels are the Pearson correlation coefficient r , the Kendall's τ coefficient and the significance level p . In each panel, the dashed line shows the correlation when the measurement uncertainties are taken into account, while the solid line shows the correlation when we ignore the measurement uncertainties.

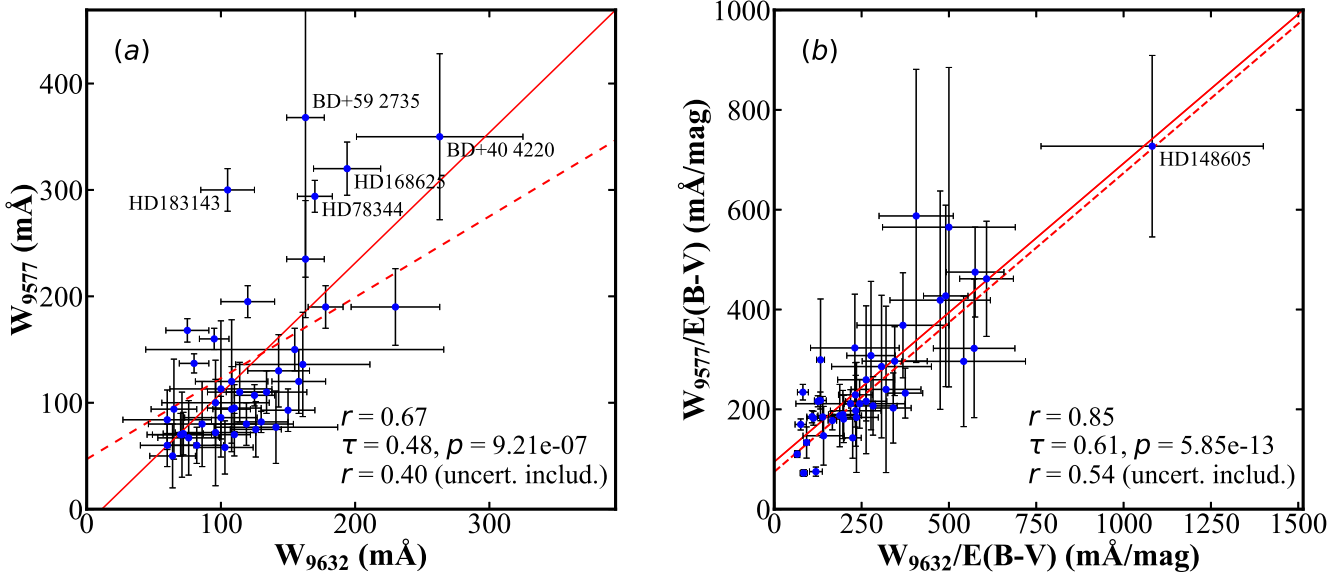


Figure 4. Left panel (a): Correlation diagram of the equivalent widths of the $\lambda 9577$ Å DIB with that of the $\lambda 9632$ Å DIB for the sample of 43 stars of Galazutdinov et al. (2021) which are listed here in Table 2. The correlation coefficient (with the measurement uncertainties included) of $r \approx 0.40$ derived here closely agrees with that derived by Galazutdinov et al. (2021; $r \approx 0.37$). Right panel (b): Same as (a) but for the *reddening-normalized* equivalent widths. It is apparent that, upon normalization, the correlation appreciably improves. The correlation coefficients largely remain unchanged if HD 148605, an outlier, is excluded. In each panel, the dashed line shows the correlation when the measurement uncertainties are considered, while the solid line shows the correlation when the measurement uncertainties are ignored.

board different telescopes. They found that, with a correlation coefficient of $r \approx 0.37$ (with the measurement uncertainties included), the equivalent widths of the $\lambda 9577$ Å DIB are poorly correlated with that of the $\lambda 9632$ Å DIB. We re-analyze the correlation and derive an uncertainty-included

correlation coefficient of $r \approx 0.40^6$ ($r \approx 0.67$ if we ignore

⁶ The small difference in the correlation coefficient r between ours and that of Galazutdinov et al. (2021) probably arises from the fact that the sight lines we consider (see Table 2) may not

Table 2. Stellar Parameters and the Equivalent Widths of the $\lambda 9577 \text{ \AA}$ DIB (W_{9577}) and $\lambda 9632 \text{ \AA}$ DIB (W_{9632}) for the 43 Stars of Galazutdinov et al. (2021).

Target Star	Spectral Type	B^a (mag)	V^a (mag)	$(B - V)_0^b$ (mag)	$E(B - V)^c$ (mag)	W_{9577} (mÅ)	W_{9632} (mÅ)
BD-14 5037	B1.5Ia	9.72	8.41	-0.17	1.48	125±15	107±10
CD-32 4348	B3Ia	10.05	9.19	-0.13	0.99	75±16	168±11
BD+40 4220	O6.5-7f+O5.5-6f	10.79	9.185	-0.29	1.90	263±62	350±78
BD+59 2735	B0Ib	10.89	9.88	-0.22	1.23	163±14	368±150
Cyg OB2 No. 7	O3If	12	10.55	-0.31	1.76	163±14	235±55
HD23180	B1III	3.88	3.83	-0.21	0.26	141±46	77±34
HD27778	B	6.499	6.337	-0.11	0.27	64±17	50±30
HD36861	O8III	3.48	3.47	-0.26	0.27	71±22	70±40
HD37022	O7Vp	5.15	5.13	-0.29	0.31	72±15	71±20
HD37041	O9.5IVp	6.3	6.39	-0.31	0.22	108±14	94±40
HD40111	B0/1II/III	4.76	4.82	-0.22	0.16	76±23	67±35
HD54662	O6.5Vz(n)+O7.5Vz	6.24	6.21	-0.29	0.32	60±20	60±20
HD57061	O9II	4.25	4.4	-0.31	0.16	65±17	94±47
HD76341	O9.2IV	7.392	7.163	-0.28	0.51	134±30	110±20
HD78344	O9.5/B0(Ib)	10.12	9	-0.24	1.36	170±13	294±15
HD80077	B2Ia+e	10.29	9	-0.16	1.45	95±11	160±10
HD91824	O7V((f))z	8.11	8.14	-0.29	0.26	60±33	84±28
HD104705	B0III/IV	9.56	9.11	-0.23	0.68	96±40	100±40
HD113904	WC5+B0III	5.5	5.53	-0.23	0.20	100±38	113±64
HD136239	B2Iae	8.86	7.95	-0.16	1.07	120±20	195±15
HD144470	B1V	3.92	3.97	-0.23	0.18	103±21	58±25
HD145502	B2V	4.05	4	-0.21	0.26	158±20	120±30
HD147165	O9.5(V)+B7(V)	3.02	2.89	-0.27	0.4	230±33	190±36
HD147888	B3/4V	7.05	6.74	-0.18	0.49	110±12	70±20
HD148379	B2Iab	5.95	5.37	-0.16	0.74	80±11	137±9
HD148605	B3V	4.72	4.79	-0.18	0.11	119±35	80±20
HD148937	O6f?p	7.12	6.71	-0.31	0.72	143±23	130±34
HD149038	O9.7Iab	4.99	4.94	-0.24	0.29	100±27	86±20
HD149757	O9.2IVnn	2.58	2.56	-0.28	0.30	96±30	72±50
HD150136	O3.5-4III(f*)+O6IV	5.78	5.65	-0.26	0.39	108±27	120±58
HD151804	O8Iaf	5.29	5.22	-0.3	0.37	126±19	75±26
HD152408	O8Iape	5.92	5.77	-0.3	0.45	110±20	95±22
HD152424	OC9.2Ia	6.69	6.27	-0.27	0.69	161±50	136±49
HD153919	O6Iafcp	6.78	6.51	-0.31	0.58	114±24	110±28
HD155806	O7.5V((f))z(e)	5.52	5.53	-0.29	0.28	86±40	80±40
HD167264	O9.7Iab	5.42	5.37	-0.24	0.29	82±20	60±17
HD167971	O8Iaf(n)+O4/5	8.27	7.5	-0.3	1.07	178±13	190±20
HD168625	B6Iap	9.78	8.37	-0.06	1.47	194±25	320±25
HD169454	B1Ia	7.61	6.71	-0.19	1.09	130±20	82±10
HD170740	B2/3I	5.96	5.72	-0.16	0.40	150±20	93±20
HD183143	B6Ia	8.08	6.86	-0.06	1.28	105±20	300±20
HD184915	B0.5IIIIn	4.93	4.96	-0.22	0.19	70±25	70±20
HD190603	B1.5Ia	6.19	5.65	-0.17	0.71	155±111	150±20

^a B and V photometric magnitudes taken from <http://cdsportal.u-strasbg.fr/>.

^b Intrinsic colors $(B - V)_0$ taken from Wegner (2014).

^c Color excesses $E(B - V) \equiv (B - V) - (B - V)_0$.

the measurement uncertainties; see Figure 4a). However, as discussed earlier, the relation between two DIBs could be affected by their common dependence on $E(B - V)$. To cancel out the common dependence on $E(B - V)$, we normalize the equivalent widths of both DIBs by $E(B - V)$ and

be exactly the same as those considered by Galazutdinov et al. (2021); indeed, it is not very clear which sight lines were examined in Galazutdinov et al. (2021).

re-examine their correlation. Figure 4b shows the correlation between $W_{9577}/E(B - V)$ and $W_{9632}/E(B - V)$ for the 43 lines of sight of Galazutdinov et al. (2021). With a Pearson correlation coefficient of $r \approx 0.85$ ($r \approx 0.54$ if the measurement uncertainties are taken into account) and a Kendall correlation coefficient of $\tau \approx 0.61$ at a significance level of $p \approx 5.85 \times 10^{-13}$, the correlation between $W_{9577}/E(B - V)$ and $W_{9632}/E(B - V)$ is considerably tighter than that between W_{9577} and W_{9632} . Therefore,

we believe that these two DIBs of the sample of Galazutdinov et al. (2021) are also correlated. The mean ratio of $W_{9632}/E(B - V) : W_{9577}/E(B - V) \approx 0.90$ agrees well with the experimental band ratio of ~ 0.84 of gas-phase C_{60}^+ (Campbell & Maier 2018).

4 CONCLUSION

We have searched for the DIBs at $\lambda 9632 \text{ \AA}$, $\lambda 9577 \text{ \AA}$, $\lambda 9428 \text{ \AA}$, $\lambda 9365 \text{ \AA}$ and $\lambda 9348 \text{ \AA}$ which are attributed to C_{60}^+ in the ESO VLT/X-shooter spectral data archive. We have identified 25 stars along the lines of sight to which all these DIBs (except the $\lambda 9348 \text{ \AA}$ DIB, the weakest absorption band in the experimental spectrum of gas-phase C_{60}^+) are seen in the X-shooter spectra. To avoid the MgII stellar contamination to the $\lambda 9632 \text{ \AA}$ DIB, we focus on a subsample of nine O and B0 stars in which the MgII stellar lines are absent or very weak. It is found that, after normalized by reddening (to eliminate their common correlation with the density of interstellar clouds), the equivalent widths of the $\lambda 9632 \text{ \AA}$ and $\lambda 9577 \text{ \AA}$ DIBs are well correlated, whereas the X-shooter spectra for the $\lambda 9428 \text{ \AA}$ and $\lambda 9365 \text{ \AA}$ DIBs are too noisy to allow any reliable quantitative analysis. We conclude that the correlation found between the strengths of the $\lambda 9632 \text{ \AA}$ and $\lambda 9577 \text{ \AA}$ DIBs, the strongest absorption bands in the experimental spectrum of gas-phase C_{60}^+ , supports C_{60}^+ as the carrier of these DIBs.

ACKNOWLEDGEMENTS

We thank K.J. Li, A.N. Witt, X.J. Yang and the anonymous referee for helpful suggestions and comments. TPN and FYX are supported in part by the Joint Research Funds in Astronomy U2031114 under cooperative agreement between the National Natural Science Foundation of China and Chinese Academy of Sciences and the CCST Milky Way Survey Dust and Extinction Project. AL is supported in part by NSF AST-1816411.

DATA AVAILABILITY

The data underlying this article will be shared on reasonable request to the corresponding authors.

REFERENCES

Berné, O., Mulas, G., & Joblin, C. 2013, *A&A*, 550, 4
 Cami, J., Bernard-Salas, J., Peeters, E., & Malek, S. 2010, *Science*, 329, 1180
 Campbell, E. K., Holz, M., Gerlich, D., & Maier, J. P. 2015, *Nature*, 523, 322
 Campbell, E. K., Holz, M., & Maier, J. P. 2016a, *ApJ*, 822, 17
 Campbell, E. K., Holz, M., & Maier, J. P. 2016b, *ApJL*, 826, L4
 Campbell, E. K., & Maier, J. P. 2018, *ApJ*, 858, 36
 Cordiner, M. A., Linnartz, H., Cox, N. L. J., et al. 2019, *ApJ*, 875, L28
 Désert, F. X., Jenniskens, P., & Dennefeld, M. 1995, *A&A*, 303, 223
 Fan, H., Hobbs, L. M., Dahlstrom, J. A., et al. 2019, *ApJ*, 878, 151

Fitzpatrick, E.L., & Massa, D. 1988, *ApJ*, 328, 734
 Foing, B. H., & Ehrenfreund, P. 1994, *Nature*, 369, 296
 Fulara, J., Jakobi, M., & Maier, J. P. 1993, *Chem. Phys. Lett.*, 211, 227
 García-Hernández, D. A., Manchado, A., García-Lario, P., Stanghellini, L., Villaver, E., Shaw, R. A., Szczerba, R., & Perea-Calderón, J. V. 2010, *ApJ*, 724, 39
 García-Hernández, D. A., Iglesias-Groth, S., Acosta-Pulido, J. A., Manchado, A., García-Lario, P., Stanghellini, L., Villaver, E., Shaw, R. A., & Cataldo, F. 2011, *ApJL*, 737, 30
 Galazutdinov, G. A., Shimansky, V. V., Bondar, A., Valyavin, G., & Krelowski, J. 2017, *MNRAS*, 465, 3956
 Galazutdinov, G. A., Valyavin, G., Ikhsanov, N. R., & Krelowski, J. 2021, *AJ*, 161, 127
 Gatchell, M., Martini, P., Laimer, F., Goulart, M., Calvo, F., & Scheier, P. 2019, *Faraday Discussion*, 217, 276
 Heger, M. L. 1922, *Lick. Obs.*, 10, 141
 Hrodmarsson, H.R., Garcia, G.A., Linnartz, H., & Nahon, L. 2020, *Phys. Chem. Chem. Phys.*, 22, 13880
 Kausch, W., Noll, S., Smette, A., et al. 2015, *A&A*, 576, A78
 Kroto, H. W., Heath, J. R., O'Brien, S. C., & Smalley, R. E. 1985, *Nature*, 318, 1622
 Lallement, R., Cox, N.L.J., Cami, J., et al. 2018, *A&A*, 614, A28
 Léger, A., d'Hendecourt, L., Verstraete, L., et al. 1988, *A&A*, 203, 145
 Li, A. 2009, in *Small Bodies in Planetary Sciences*, ed. I. Mann, A. Nakamura, & T. Mukai (Berlin: Springer), 167
 Li, K.J., Li, A., & Xiang, F.Y. 2019, *MNRAS*, 489, 708
 Linnartz, H., Cami, J., Cordiner, M., et al. 2020, *J. Mol. Spectrosc.*, 367, 111243
 Lykhin, A., Ahmadvand, S., & Varganov, S.A. 2019, *J. Phys. Chem. Lett.*, 10, 115
 McCabe, M. 2019, *Astronomy & Geophysics*, 60, 4.29
 Merrill, P. W., & Wilson, O. C. 1938, *ApJ*, 87, 9
 Moutou, C., Krelowski, J., d'Hendecourt, L., & Jamrozczak, J. 1999, *A&A*, 351, 680
 Nielbock, M., Chini, R., Jütte, M., & Manthey, E. 2001, *A&A*, 377, 273
 Omont, A. 2016, *A&A*, 590, 52
 Rawlings, M. G., Adamson, A. J., & Kerr, T. H. 2014, *ApJ*, 796, 58
 Ramírez-Tannus, M. C., Cox, N. L. J., Kaper, L., & de Koter, A. 2018, *A&A*, 620, A52
 Sarre, P. J. 2006, *J. Mol. Spectrosc.*, 238, 1
 Seab, C. G., & Snow, T. P. 1984, *ApJ*, 277, 200
 Sellgren, K., Werner, M. W., Ingalls, J. G., Smith, J. D. T., Carleton, T. M., & Joblin, C. 2010, *ApJ*, 722, 54
 Smette, A., Sana, H., Noll, S., et al. 2015, *A&A*, 576, A77
 Snow, T. P., Seab, C. G., & Joseph, C. L. 1988, *ApJ*, 335, 185
 Spieler, S., Kuhn, M., Posteler, J., et al. 2017, *ApJ*, 846, 168
 Strelnikov, D., Kern, B., & Kappes, M. M. 2015, *A&A*, 584, A55
 Vernet, J., Dekker, H., D'Odorico, S., et al. 2011, *A&A*, 536, A105
 Wegner, W. 2014, *AcA*, 64, 261
 Walker, G. A. H., Bohlender, D. A., Maier, J. P., & Campbell, E. K. 2015, *ApJ*, 812, L8
 Walker, G. A. H., Campbell, E. K., Maier, J. P., Bohlender, D., & Malo, L. 2016, *ApJ*, 831, 130
 Walker, G. A. H., Campbell, E. K., Maier, J. P., & Bohlender, D. 2017, *ApJ*, 843, 56
 Witt, A. N., Bohlin, R. C., & Stecher, T. P. 1983, *ApJ*, 267, L47
 Xiang, F.Y., Li, A., & Zhong, J.X. 2011, *ApJ*, 733, 91
 Xiang, F.Y., Li, A., & Zhong, J.X. 2017, *ApJ*, 835, 107
 Zhang, Y., & Kwok, S. 2011, *ApJ*, 730, 126

This paper has been typeset from a \LaTeX file prepared by the author.